Preparation and properties of silicon nanocrystals by femtosecond laser in solution doped with Boron

Preparation and properties of silicon nanocrystals by femtosecond laser in solution doped with Boron

Kuntian Ren, Huilian Hao*, Yingxiong Zhang, Jiaqi Wu, Wenbin Yin, Wentao Zhao

School of Material Engineering, Shanghai University of Engineering Science, Shanghai, China

*Corresponding author email: sulee8866@126.com

Abstract: Colloidal silicon (Si) nanocrystals (NCs) were made via femtosecond laser ablation of silicon power in 1-octadecene mixed with boron oxide. It is reflected that nano-particles dispersed evenly in 1-octadecene without aggregation via High resolution transmission electron microscopy (HRTE). Phenomenon with a redshift and an asymmetrical widening of Raman peak is demonstrated by Raman analysis. Fourier transform infrared (FTIR) spectra directly show that oxide molecules and organic chains have terminated the surfaces of Si nanoparticles. According to Raman spectra and FTIR spectra, we can infer that boron atoms are incorporated into Si NCs or connected with Si NCs surfaces. In the light of room-temperature photoluminescence (PL) spectra, the PL peeks remain unchanged, moreover, PL intensity were found to reduce with increasing amount of boron oxide.

1. Introduction

Recently, owing to employing outstanding characteristic of quantum confinement effect, semiconductor nano-particles have been comprehensively applied to potential optoelectronic and biological applications. For example LED lamp [1], transistors [2], bioimaging tools [3, 4] and solar cells [5]. It is necessary to make Silicon (Si) nanocrystals (NCs) doped so that it can adapt to various applications [6-8]. The structural transformation, electrical, optic and magnetic nature of doped Si NCs have been deliberated by a lot of theoretical efforts [9]. Either in theory or experiment, Nakamura. *et al.* have reported the doped behavior and photoluminescence character of Si NCs which was incorporated by phosphorus (P) or boron (B) separately as well as co-doped by P and B [10]. Compared to bulk counterpart, the doped behaviors by P, B or co-doped via P and B of Si NCs were seemed to be complex. Moreover, it is reported that the efficiencies of doping were quite debased [11-13]. In this paper, we mainly focus on research the structural transformation and optic character of boron doped Si NCs which are fabricated by the laser ablation in liquids.

2. Experiments and results

Fabrication processing of the Si NCs was expounded in detail as foregone research14]. In this work. To be brief, the porous silicon powder and boron oxide were mixed in 1-octadecence (20 ml), wich was ultrasonically for 30min. Subsequently, femtosecond (fs) pulsed Ti/sapphire laser (100fs pulse duration, 80 MHz frequency) was carried out at 800 nm to perform the laser ablation. The porous

silicon powder were 40 mg, and the corresponding amount of boron oxide were 10, 15, 20, 25 mg, and then were named with Sx (x=1, 2, 3, 4) for laser ablation time at 1.0 h.

The fabrication and structure of the samples were confirmed via high resolution transmission electron microscopy (TF20, Joel). Jobin Yvon LabRAM HR 800 UV were used to measure Raman scattering spectra. Fourier transform infrared (FTIR) spectra were performed within 400-4000 cm^{-1} range at NEXUS 670. The photoluminescence (PL) spectra were preserved by Edinburgh Instruments FLS920.

Figures 1(a) and (b) show TEM and the size distributions for S1 respectively. No three-dimensional agglomerates take shape, implying that the spherical Si nanoparticles are well dispersed. The lattice fringes for HRTEM in the section of TEM are assigned to be the (111) plane of Si crystals (~0.33 nm). Compared with un-doped Si NCs, lattice fringes of Si (111) was amplified, this is supposed to be the result of structural defects related to interstitial B [9]. The selected area electron diffraction (SAED) is displayed in the bottom-right of figure 1(a) as well，showing the crystallinity [14]. The average particle size is around 3.68 nm.

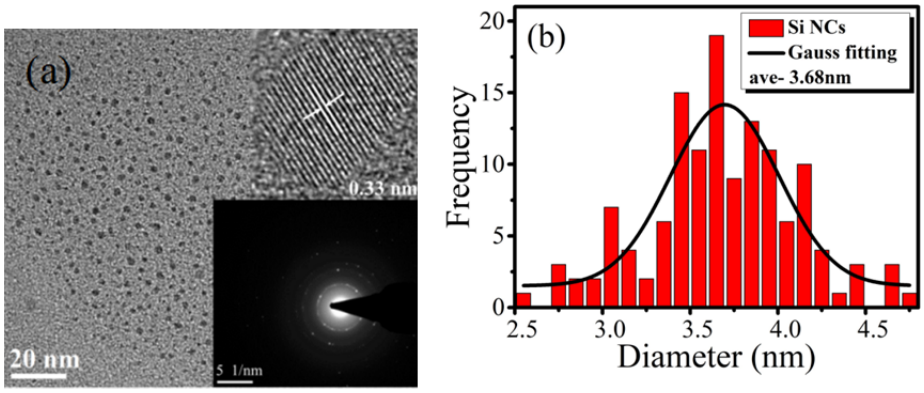

Figure 1 (a) TEM (b) size distribution of S1. Inset: a typical HRTEM image of a Si NC(upper)and SAED(lower）.

The Raman spectra of all samples prepared in 1-octadecence were displayed in Figure 2(a). As we can see, there are two visible peeks. The peek located at 640 cm^{-1} is ascribed to B-Si bonds, implying that B has been incorporated into Si NCs [13]. All of the samples possess this peek and keep unchanged. It is clearly shown that the Raman peak position of S1-S4 locate at 518.4, 517.5, 515.5, and 511 cm^{-1}, respectively, which is red-shifted with respect to bulk silicon crystalline (520 cm^{-1}). The red-shift is ascribed to the fact that B impurities participated the enlargement of tensile strain for Si-Si bond length, generating tensile stress and structural alteration in Si NCs [13]. Full width half maximum (FWHM) of samples is 5.0, 6.2, 4.7, and 4.2 cm^{-1}, respectively. Downshift along with the widening of FWHM further confirms the effectiveness of phonon confinement effect [14]. Relationship of downshift ($\Delta\nu$) with Si NCs size can be reflected via the phenomenological law [8] : $\Delta\nu = -19.856 / d^{1.586}$. Here, the average size is calculated to be ~ 4.81, 3.68, 2.52, and 1.63 nm.

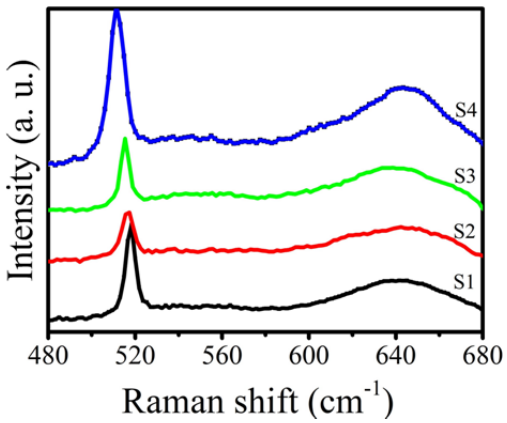

Figure 2 Raman spectra of all samples.

Fourier transform infrared spectra (FTIR) for all samples were displayed at Figure 3(a), revealing bonding property on Si NCs surface. It is identified that the bonds at 2853 and 2923 cm^{-1} are symmetric and asymmetric C-H_2 stretching [15]. Bonds at 880, 930, 1080, 1457, 1630cm^{-1} and 2245cm^{-1} are Si-C symmetric, B-O-Si, Si-O-Si asymmetric stretching mode, B-O-B stretching modes, Si-OH vibration modes and OSi-H_X the stretching modes respectively [14,16,17]. The formation of alkyl-related bonds arise from the cycloaddition chemistry reaction in target solution, demonstrating that Si NCs are terminated with alkyl-related molecule. Passivation with alkyl-related molecule is identified to result in the less non-radiative centers, as well as smaller non-radiative rate [18]. It is reflected that oxygen dissolved in solution have been partly oxidized the Si NCs surfaces via Si-O-Si bonds. The emergence of B-O-Si bond indicates B atoms may be contact with SiNCs with oxide formation. It is accepted that water molecules may separate the Si-Si bonds and then substitute with Si-H and Si-OH passivation. The Si-OH passivation may further condense and then terminate with Si-O-Si or Si=O bands [16]. Stretching mode of OSi-H_X is ascribed to back-bond oxidation for Si-H stretching [16].

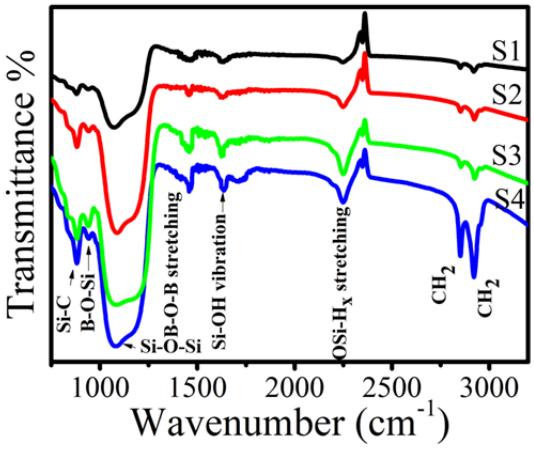

Figure 3 Fourier transform infrared spectra for all samples.

Figure 4 displays the PL spectra under 325 nm excitation wavelength. The emission peaks of S1-S4 at 469 nm (2.64 eV), 488 nm (2.54 eV) and 536 nm (2.31 eV) remain unchanged, moreover, the PL intensity decrease gradually with the increasing amount of boron oxide. The reasons for the relationship between PL intensity and boron concentration are discussed as following. (i) It is confirmed that the considerable size diversity between boron and Si atoms will make boron form flawed tensile strain defects. Covalent radius for Si and boron are 0.117 and 0.088nm, respectively.

When Si were replaced by boron atoms, the considerable size diversity for Si and boron atoms gives rise to the structural flaw of Si NCs which may be worse with increasing boron concentration. The imperfect structural defects lead to non-radiative recombination centers, which reduce PL signal with increasing boron concentration. (ii) The non-radiative Auger recombination procedures are supposed to enhance for more boron atoms incorporated into Si NCs [19].

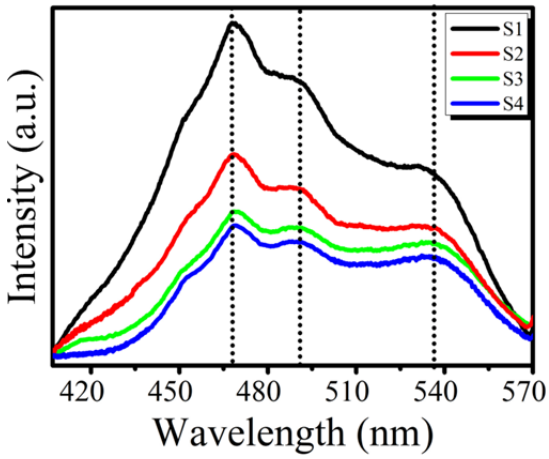

Figure 4 PL spectra of S1-S4

3. Conclusion

We draw a conclusion that B-doped Si NCs have been made via femtosecond laser ablation in 1-octadecence. Structure as well as optical characters of B-doped Si NCs which are doped for various amount of B were investigated. Analyzed from the HRTEM, Raman spectra, we identify that B atoms have been incorporated into Si NC and have influenced the structure and optic characters of Si NCs. Moreover, FTIR measurements show that organic molecules and oxygen have well terminated the surface of Si NCs. Form room-temperature PL spectra, we find that the PL intensity reduces gradually with increasing amount of boron oxide. It is confirmed that the flawed defects and non-radiative auger recombination induced by doping B atoms into Si NCs have been attributed to decreasing PL intensity.

Acknowledgments

This work was financially supported by the National Natural Science Foundation of China (Grant No. 11504229) and Innovation Training for National College Students (201810856021).

References

[1] Tan. Z, Zhang. F, Zhu. T, Xu. J, Wang. A. Y, Dixon. J. D, Li. L, Zhang. Q, Mohney. S. E, Ruzyllo. J. Bright and color-saturated emission from blue light-emitting diodes based on solution-processed colloidal nanocrystal quantum dots. Nano Lett. 7 (2007) 3803−3807.

[2] Talapin. D. V, Murray. C. B. PbSe nanocrystal solids for n- and p-channel thin film field-effect transistors. Science 310 (2005) 86−89.

[3] Michalet. X, Pinaud. F. F, Bentolila. L. A, Tsay. J. M, Doose. S, Li. J. J, Sundaresan. G, Wu. A. M, Gambhir. S. S, Weiss. S. Quantum dots for live cells, in vivo Imaging, and diagnostics. Science 307 (2005) 538−544.

[4] Cai. W, Shin. D. W, Chen. K, Gheysens. O, Cao. Q, Wang. S. X, Gambhir. S. S, Chen.X. Peptide-labeled near-infrared quantum dots for imaging tumor vasculature in living subjects.

Nano Lett. 6 (2006) 669−676.

[5] Gur. I, Fromer. N. A, Geier. M. L, Alivisatos. A. P. Air-stable all-inorganic nanocrystal solar cells processed from solution. Science 310 (2005) 462−465.

[6] Pi. X. D. Doping silicon nanocrystals with boron and phosphorus. J. Nanomater 2012 (2012) 912903.

[7] Carvalho. A, Öberg. S, Rayson. M. J and Briddon. P. R. Electronic properties, doping, and defects in chlorinated silicon nanocrystals Phys. Rev. B 86 (2012) 045308.

[8] Cantele. G, Degoli. E, Luppi. E, Magri. R, Ninno. D, Iadonisi. G and Ossicini. S First-principles study of n- and p-doped silicon nanoclusters Phys. Rev. B 72 (2005) 113303.

[9] Ni. Z, Pi. X. D, Ali. M, Shu. Z, Tomohiro. N and Deren. Y. Freestanding doped silicon nanocrystals synthesized by plasma. J. Phys. D: Appl. Phys. 48 (2015) 314006.

[10] Nakamura T, Adachi S, Fujii M, K. Miura, and S. Yamamoto. Phosphorus and boron codoping of silicon nanocrystals by ion implantation: photoluminescence properties. Phys. Rev. B: Condens. Matter 85 (2012) 435-441.

[11] A. R. Stegner, R. N. Pereira, K. Klein, R. Lechner, R. Dietmueller, M. S. Brandt, M. Stutzmann,and H. Wiggers. Electronic transport in phosphorus-doped silicon nanocrystal networks Phys. Rev. Lett.100 (2008) 026803.

[12] S. Gutsch, A. M. Hartel, D. Hiller, N. Zakharov, P. Werner, and M. Zacharias. Doping efficiency of phosphorus doped silicon nanocrystals embedded in a SiO_2 matrix. Appl. Phys. Lett. 100 (2012) 233115.

[13] Li. D. K, J. Y. C , P. Z, S. D, X. J, L. W and C. K. J. The phosphorus and boron co-doping behaviors at nanoscale in Si nanocrystals/SiO_2 multilayers. Appl. Phys. Lett. 110 (2017) 233105.

[14] V. Nguyen, L. H. Yan, J. H. Si and X. Hou. Femtosecond laser-induced size reduction of carbon nanodots in solution: Effect of laser fluence, spot size, and irradiation time. J. Appl. Phys. 117 (2015) 084304.

[15] J. Zou, R. K. Baldwin, K. A. Pettigrew and S. M. Kauzlarich. Solution synthesis of ultrastable luminescent siloxane-coated silicon nanoparticles. Nano Lett. 4 (2004) 1181-1186.

[16] Mariotti. D, Švrček. V, Hamilton J. W. J, Schmidt. M and Kondo. M. Silicon nanocrystals in liquid media: optical properties and surface stabilization by microplasma-induced non-equilibrium liquid chemistry. Adv. Funct. Mater. 22 (2012) 954-964.

[17] Sasaki. M, Kano. S, Sugimoto. H, Imakita.K, M. Fujii. Surface structure and current transport property of boron and phosphorous co-doped silicon nanocrystals. J. Phys. Chem. C 120 (2016) 195-200.

[18] S. Godefroo, M. Hayne, M. Jivanescu, A. Stesmans, M. Zacharias, O. I. Lebedev, G. Van Tendeloo and V. V. Moshchalkov. Classification and control of the origin of photoluminescence from Si nanocrystals, Nat. Nanotechnology 3 (2008) 174-178.

[19] X. J. Hao, E. C. Cho, C. Flynn, Y. S. Shen, S. C. Park, G. Conibeer, M. A. Green. Synthesis and characterization of boron-doped Si quantum dots for all-Si quantum dot tandem solar cells. Sol. Energy Mater. Sol. Cells 93 (2009) 273-279.